

000
001
002
003
004
005
006
007
008
009
010
011
012
013
014
015
016
017
018
019
020
021
022
023
024
025
026
027
028
029
030
031
032
033
034
035
036
037
038
039
040
041
042
043
044
045
046
047
048
049
050
051
052
053

HIPo: SELF-HINT POLICY OPTIMIZATION FOR RLVR

Anonymous authors

Paper under double-blind review

ABSTRACT

Reinforcement Learning from Verifiable Rewards (RLVR) is a promising method for enhancing the complex problem-solving abilities of large language models (LLMs). This is particularly evident in domains requiring long-horizon reasoning and precise execution, such as solving complex mathematical problems where solutions hinge on a fragile sequence of tool-based actions. However, current approaches are often crippled by two interconnected issues: the near-miss problem, where sparse rewards nullify the learning signal for almost-correct attempts, and the resulting exploration stagnation, which prevents the model from discovering better solutions. To address these challenges, we introduce HiPO (Hint-guided Policy Optimization), a novel RLVR framework that enables the agent to learn from its own rare successes. Our core insight is to capture an occasional successful trajectory within a training batch and repurpose its initial correct steps as an on-policy “hint”. This process transforms a single, stochastically-found success into a dense contrastive learning signal, effectively allowing the model to teach itself how to overcome the near-miss problem and break exploration stagnation. On a challenging suite of five mathematical reasoning benchmarks, HiPO improves the average avg@32 by +5.0 percentage points (pp) over the strong GRPO baseline. This improvement is driven by substantial absolute point gains on challenging datasets, including +10.3 pp on CMIMC 2025, +4.9 pp on BRUMO 2025, +4.6 pp on AIME 2024, and +3.1 pp on AIME 2025. Furthermore, HiPO demonstrates a new exploration paradigm, repurposing rare successes into reusable guidance to significantly accelerate skill acquisition for complex tasks, establishing a more efficient and scalable path for models to autonomously master intricate reasoning.

1 INTRODUCTION

A central ambition in artificial intelligence is to create agents capable of acquiring complex reasoning skills autonomously, moving beyond the reliance on curated expert data (DeepSeek, 2025; Lambert et al., 2024). Reinforcement Learning from Verifiable Rewards (RLVR) marks a promising step towards this vision, enabling Large Language Models (LLMs) to learn from outcome-based feedback in domains like advanced mathematics (Shao et al., 2024; DeepSeek, 2025). However, this pursuit confronts a fundamental paradox rooted in the very nature of complex problem-solving. Success often depends on a fragile sequence of self-reflection (Renze & Guven, 2024) and tool-integrated reasoning (Feng et al., 2025; Li et al., 2025b), making a correct solution an exceptionally rare event. This fragility exposes a critical flaw in current RLVR frameworks: a *brittleness of the learning signal*.

This signal brittleness manifests in two interconnected challenges. The first is the *near-miss problem*: a nearly-perfect trajectory receives the same sparse, negative reward as a complete failure, thereby penalizing correct intermediate reasoning steps through flawed credit assignment. Consequently, this leads to the second, more debilitating challenge: *exploration stagnation*. The consistent punishment for near-misses disincentivizes any deviation from simple, suboptimal strategies, preventing the very breakthroughs in capability the learning process is meant to foster (Cui et al., 2025; An et al., 2025; Cheng et al., 2025). This is further exacerbated by *signal collapse*, a scenario where uniform rewards within a training batch cause the policy gradient to vanish entirely (Yu et al., 2025; Xu & Ding, 2025). In essence, the agent cannot learn from its successes if those successes are statistically impossible to discover.

To make this exploration challenge concrete, consider a motivating example. As shown in Figure 1, a baseline model without guidance struggles to generate correct trajectories. However, when provided with a partial correct solution as a “hint”, its performance improves dramatically, transforming the distribution from near-certain failure to high-probability success. This stark contrast suggests the primary bottleneck is not the model’s intrinsic reasoning ability, but the *discovery* of a valid reasoning path. This begs the critical question: can a model learn to provide these crucial hints for itself, *bootstrapping* its own learning from its own rare successes?

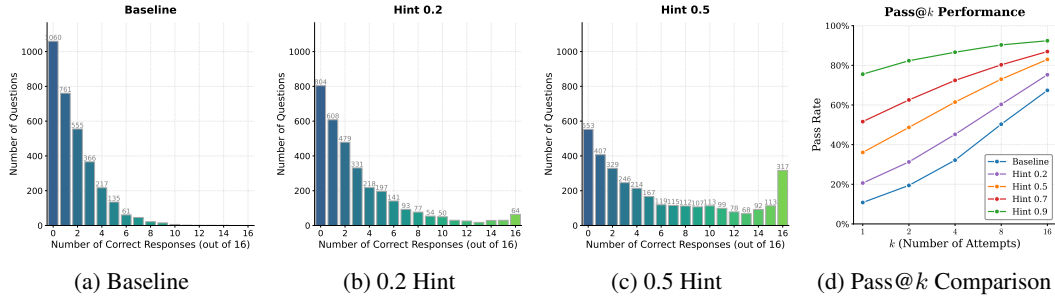


Figure 1: (a-c) show as the hint ratio (the proportion of the trajectory as a prefix) increases, the correct solutions improves. (d) compares the pass@k performance for different hint ratios.

To answer this question, we introduce Hint-guided Policy Optimization (HiPO), a framework that operationalizes a new paradigm: **Endogenous Self-Hint**. The core insight is that a single, stochastically-found success is not merely an endpoint to be rewarded, but a rich source of curriculum to be exploited. HiPO captures these rare successful trajectories and repurposes their initial correct steps as on-policy “hints”. This process transforms the intractable task of *end-to-end discovery* into a more manageable one of *guided completion*. By juxtaposing the policy’s unaided exploration with its hint-guided exploration, HiPO forges a dense and powerful contrastive learning signal from sparse rewards. It directly resolves the near-miss problem by rewarding valid reasoning prefixes, and by providing a trustworthy path forward, it shatters exploration stagnation, guiding the policy toward mastering more complex reasoning patterns.

Our main contributions are:

- We propose HiPO, a new framework that materializes the concept of endogenous self-hint. It leverages policy’s own rare successes as on-policy hints to create a robust, contrastive learning signal, converting sparse rewards into a dense, self-generated curriculum.
- HiPO significantly outperforms a strong GRPO baseline on five challenging mathematical reasoning benchmarks, achieving a +5.0 pp average improvement in avg@32. The gains are particularly substantial on difficult datasets, including CMIMC 2025 (+10.3 pp) (Balunović et al., 2025), BRUMO 2025 (+4.9 pp) (Balunović et al., 2025), and AIME 2024 (+4.6 pp).
- We provide empirical evidence that HiPO successfully counteracts exploration stagnation. Through analysis of training dynamics, we show that it maintains higher policy entropy and fosters longer, more complex tool-use sequences, confirming that our self-hint mechanism enables more sophisticated reasoning.

These results highlight HiPO as an efficient and scalable paradigm for autonomous learning. By enabling models to repurpose their own successes into reusable guidance, our work provides a bootstrapped pathway to mastering complex tasks, accelerating progress towards more capable and independent AI systems.

2 RELATED WORK

A prominent baseline within RLVR (Lambert et al., 2024; DeepSeek, 2025) is Group Relative Policy Optimization (GRPO) (Shao et al., 2024), which simplifies policy optimization by forgoing a critic network and instead normalizing rewards across a group of concurrently generated responses.

108 However, this group-based approach is crippled when rewards are sparse; if all responses in a training
 109 batch fail, the resulting advantage is zero, nullifying the learning signal. To mitigate this, meth-
 110 ods like DAPO (Yu et al., 2025) enhance GRPO with engineering treatments such as dynamic sam-
 111 pling, which forces the generation process to continue until a non-zero advantage is found. Despite
 112 these improvements, such approaches are fundamentally reactive; they can only refine the learn-
 113 ing signal if at least one successful trajectory is stochastically discovered within a group, failing to
 114 address the core exploration problem when success is exceptionally rare.

115 Moving beyond purely algorithmic modifications, another line of work injects external guidance to
 116 scaffold learning. QuestA (Li et al., 2025a) and StepHint (Zhang et al., 2025), for instance, augment
 117 prompts with partial solutions or stepwise hints derived from *stronger teacher models* or *existing*
 118 *datasets* of OpenR1-Math-220K (OpenR1, 2025). While effective at creating a denser reward signal,
 119 this reliance on external, *off-policy* guidance creates a dependency on pre-existing knowledge and
 120 does not represent autonomous learning from the agent’s own experience. Our work, HiPO, provides
 121 a novel synthesis to overcome these limitations. It addresses the sparse reward problem like hint-
 122 based methods, but does so by creating hints that are both *endogenous* and *on-policy*. By capturing
 123 a rare success within a training batch and repurposing its initial correct steps as a hint for the entire
 124 group, HiPO enables the model to teach itself, transforming a single stochastic success into a dense,
 125 reusable learning signal without depending on external teacher models.

126 3 BACKGROUND

127 3.1 POLICY GRADIENT IN RLVR

130 The optimization of RLVR is fundamentally grounded in the policy gradient theorem from reinforce-
 131 ment learning (Sutton & Barto, 2018). We can formalize the sequential problem-solving process as
 132 a finite-horizon Markov Decision Process (MDP) (Puterman, 1990). For a given prompt P , serves
 133 as the initial state s_0 , the model autoregressively generates a trajectory $\tau = (o_0, o_1, \dots, o_{T-1})$, a
 134 sequence of tokens from a vocabulary \mathcal{V} . At each step t , the model’s policy π_θ defines a probability
 135 distribution over the next token o_t , conditioned on the current state s_t .

136 The policy π_θ , parameterized by the model’s weights θ , is the language model itself. In RLVR, a
 137 sparse reward $R(\tau)$ is typically assigned only at the end of a generated trajectory τ . The objective
 138 is to adjust the parameters θ to maximize the expected reward over all possible trajectories:

$$139 \quad J(\theta) = \mathbb{E}_{\tau \sim \pi_\theta}[R(\tau)]. \quad (1)$$

141 The policy gradient is optimized by computing its gradient with respect to θ , which can be estimated
 142 by sampling:

$$143 \quad \nabla_\theta J(\theta) = \mathbb{E}_{\tau \sim \pi_\theta}[R(\tau) \nabla_\theta \log \pi_\theta(\tau)]. \quad (2)$$

144 To reduce the high variance of this estimator, a state-dependent baseline $b(P)$ is subtracted from the
 145 reward $R(\tau)$ to yield a lower-variance advantage estimate, $A(\tau) = R(\tau) - b(P)$. This results in the
 146 final policy gradient update rule:

$$147 \quad \nabla_\theta J(\theta) = \mathbb{E}_{\tau \sim \pi_\theta}[A(\tau) \nabla_\theta \log \pi_\theta(\tau)]. \quad (3)$$

149 This rule guides the model to favor trajectories with positive advantages (better than average) and
 150 avoid those with negative ones, making a meaningful advantage signal crucial for effective learning.

152 3.2 GROUP RELATIVE POLICY OPTIMIZATION

153 Group Relative Policy Optimization (GRPO) is a prominent RLVR algorithm that forgoes a learned
 154 critic network, which is a key component of the PPO algorithm (Schulman et al., 2017). Instead,
 155 it constructs an empirical, on-the-fly advantage signal by generating a group of n trajectories $\mathcal{T}_j =$
 156 $\{\tau_{j,1}, \dots, \tau_{j,n}\}$ for each prompt P_j .

158 To optimize, GRPO maximizes an objective function based on an importance sampling ratio. For a
 159 given trajectory $\tau_{j,i} \in \mathcal{T}_j$, we define the probability ratio for each token $o_{j,i,t}$ at timestep t as:

$$161 \quad r_t^{(j,i)}(\theta) = \frac{\pi_\theta(o_{j,i,t} | P_j, o_{j,i,<t})}{\pi_{\theta_{\text{old}}}(o_{j,i,t} | P_j, o_{j,i,<t})}, \quad (4)$$

162 where $o_{j,i,< t}$ represents the sequence of tokens. The objective function is defined as:
 163

$$164 \quad \mathcal{J}_{\text{GRPO}}(\theta) = \mathbb{E}_{P_j, \mathcal{T}_j} \left[\frac{1}{n} \sum_{i=1}^n \frac{1}{|\tau_{j,i}|} \sum_{t=1}^{|\tau_{j,i}|} \min \left(r_t^{(j,i)}(\theta) \hat{A}_{j,i}, \text{clip} \left(r_t^{(j,i)}(\theta), 1 - \epsilon, 1 + \epsilon \right) \hat{A}_{j,i} \right) \right]. \quad (5)$$

168
 169 GRPO’s core lies in its advantage normalization, where a single advantage $\hat{A}_{j,i}$ is computed for each
 170 trajectory $\tau_{j,i}$ and applied uniformly across all its tokens:
 171

$$172 \quad \hat{A}_{j,i} = \frac{R(\tau_{j,i}) - \mu_{\mathcal{T}_j}}{\sigma_{\mathcal{T}_j} + \epsilon_{\text{stable}}}. \quad (6)$$

173 where $\mu_{\mathcal{T}_j} = \frac{1}{n} \sum_{k=1}^n R(\tau_{j,k})$ is the mean reward of the group, and $\sigma_{\mathcal{T}_j}$ is its standard deviation.
 174 The policy is then updated using this uniform advantage signal across all time steps of the trajectory.
 175

176 However, while this design is computationally efficient, its reliance on a single outcome reward in-
 177 troduces critical flaws. The first, and for our purposes the most detrimental, is the problem of credit
 178 misassignment for fragile trajectories. In the context of complex mathematical reasoning, a trajec-
 179 tory is often “fragile”; a single error can invalidate a long sequence of correct logical steps, thereby
 180 resulting in a minimal or zero final reward. Under this reward structure, the negative feedback de-
 181 rived from this outcome is uniformly distributed across all tokens in the sequence. Consequently, the
 182 vast majority of correct and valuable reasoning steps are unduly penalized, which actively impedes
 183 the model’s acquisition of the long-form logic required for challenging problems.
 184

185 Furthermore, the reliance on the formulation in Equation 6 gives rise to another critical flaw: the
 186 signal collapse problem (Yu et al., 2025; Xu & Ding, 2025). This issue materializes in what we term
 187 a “null-signal group”, a scenario wherein all trajectories happen to share the same reward. In such
 188 cases, both the numerator ($R(\tau_{j,i}) - \mu_{\mathcal{T}_j}$) and the denominator ($\sigma_{\mathcal{T}_j}$) of the advantage calculation
 189 nullify. This inevitably results in $\hat{A}_{j,i} = 0$ for every sample, which constitutes a catastrophic loss of
 190 the learning signal that leads to the stagnation of exploration.
 191

4 THE HiPO FRAMEWORK

4.1 CORE MECHANISM: ON-POLICY HINT

195 The core mechanism of HiPO constructs a contrastive learning signal by juxtaposing the policy’s
 196 unaided exploration with its hint-guided exploration. HiPO enriches low-signal batches by using
 197 rare successes to generate high-signal replacements for completely unlearnable groups. This process
 198 unfolds in two phases for each prompt P_j within a given mini-batch.
 199

200 First, the policy attempts to solve the prompt without assistance, generating a standard Group of n
 201 trajectories, $\mathcal{T}_{\text{orig},j}$. This group faithfully reflects the model’s current capabilities.
 202

$$\mathcal{T}_{\text{orig},j} = \{\tau_1, \dots, \tau_n\} \quad \text{where} \quad \tau_i \sim \pi_{\theta}(\cdot | P_j). \quad (7)$$

203 From this initial generation, we identify specific low-performing groups as “Near-miss Groups”
 204 $\mathcal{T}_{\text{near-miss},j}$, which are defined as those where the success rate of rollouts falls below half, and “Un-
 205 learnable Groups” $\mathcal{T}_{\text{null-signal},j}$, where the reward variance is zero. The upper portion of Figure 2
 206 visually represents a $\mathcal{T}_{\text{near-miss},j}$, characterized by a high proportion of failed rollouts (red) and a
 207 scarcity of successful ones (green), which typifies the challenge in complex reasoning tasks.
 208

209 To counteract this, we employ a guided exploration strategy. First, an on-policy hint pool is con-
 210 structed from the set of all successful trajectories within the near-miss group: $\mathcal{H}_{\text{pool},j} = \{\tau \in$
 $\mathcal{T}_{\text{near-miss},j} \mid R(\tau) = 1\}$. The core of this strategy is to capitalize on these rare successes to generate
 211 a new, high-signal Hinted Group, $\mathcal{T}_{\text{hint},j}$. To ensure diversity within this new group, each trajectory
 212 is generated using a unique hint. This hint is created via a two-stage sampling process: first, a source
 213 trajectory τ_{source} is uniformly sampled from $\mathcal{H}_{\text{pool},j}$. Second, a prefix ratio p is sampled from dis-
 214 crete values in the range $[0.05, 0.45]$ with a step of 0.05 to determine a hint length $k = \lfloor p \cdot |\tau_{\text{source}}| \rfloor$.
 215 This procedure yields a unique hint, $H_{j,i} = \text{Prefix}(\tau_{\text{source}}, k)$, which represents the initial steps of
 a successful attempt. As illustrated in Figure 2, this process corresponds to randomly truncating a

216
 217
 218
 219
 220
 221
 222
 223
 224
 225
 226
 227
 228
 229
 230
 231
 232
 233
 234
 235
 236
 237
 238
 239
 240
 241
 242
 243
 244
 245
 246
 247
 248
 249
 250
 251
 252
 253
 254
 255
 256
 257
 258
 259
 260
 261
 262
 263
 264
 265
 266
 267
 268
 269

Problem
 Let ABCD be a tetrahedron such that $AB=CD= \dots$ is not divisible by the square of any prime. Find $m+n+p$.

Hint
 Okay, so I have this problem about a tetrahedron with specific edge lengths. The question is asking for ..., which is equal. Then express that

Completion
 distance in the form ... so volume is Alternatively, perhaps I can compute the ... Yes. So that's correct. So all steps are correct. So the answer is 104.
 <answer>104</answer>

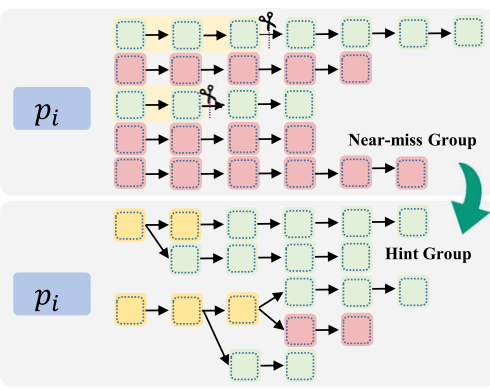


Figure 2: An illustration of the HiPO core mechanism.

successful trajectory. The final trajectory is then generated conditioned on the hint being appended to the original prompt: $\tau'_i \sim \pi_\theta(\cdot | P_j \oplus H_{j,i})$. A detailed discussion of the hint generation strategy is provided in Appendix D

The theoretical underpinning of this method is its principled resolution of sample inefficiency. A naive alternative for improving sample efficiency might involve augmenting the training data with off-policy expert trajectories drawn from a distribution π_E . This approach, however, suffers from two fundamental drawbacks. The most critical is a practical one: the requisite high-quality expert data is often prohibitively expensive or simply unavailable, as its acquisition demands either extensive manual annotation or a pre-existing, superior “teacher” model. This reliance on external supervision contrasts sharply with self-sufficient, bootstrapping methods like our own. Secondly, even if such data were accessible, its introduction engenders a significant distributional mismatch between the agent’s policy π_θ and the expert policy π_E . This discrepancy is a well-documented cause of training instability, hindering reliable convergence by destabilizing the gradient estimator.

Algorithm 1 The Hint Mechanism of HiPO

Input: A prompt P , current policy π_θ , group size n .
Output: An augmented group of trajectories.

```

1: procedure GENERATEAUGMENTEDGROUP( $P, \pi_\theta, n$ )
2:    $\mathcal{T}_{\text{orig}} \leftarrow$  Generate  $n$  trajectories for  $P$  using policy  $\pi_\theta$ .
3:    $\mathcal{H}_{\text{pool}} \leftarrow \{\tau \in \mathcal{T}_{\text{orig}} \mid R(\tau) = 1\}$ .
4:   IF  $0 < |\mathcal{H}_{\text{pool}}| < n/2$  then
5:      $\mathcal{T}_{\text{hint}} \leftarrow \emptyset$ .
6:     FOR  $k = 1, \dots, n$  do
7:        $H \leftarrow \text{ExtractRandomHint}(\mathcal{H}_{\text{pool}})$ .
8:       Generate  $\tau'_{\text{new}}$  from  $P \oplus H$  and add to  $\mathcal{T}_{\text{hint}}$ .
9:     end FOR
10:    RETURN  $\mathcal{T}_{\text{hint}}$ 
11:   end IF
12: end procedure

```

Ultimately, the policy update leverages data from both the Original and Hinted groups. This transforms a potentially degenerate learning signal into a well-posed, contrastive optimization problem. This self-teaching process, formalized in Algorithm 1, is strategically activated to create this contrast precisely when it is most needed. The hint-generation phase is triggered for what we term “Near-miss Groups”: those where the success rate is greater than zero but falls below half. This targets the critical scenarios where initial successes are present but fragile, representing moments where the model is on the cusp of a breakthrough but still requires guidance. The resulting juxtaposition of the low-success-rate Original Group and the high-success-rate Hinted Group creates a highly informative advantage signal: a positive advantage reinforces the completion of nascent but promising

270 reasoning paths, as demonstrated in the Hinted Group, while a negative advantage penalizes identifiable failure modes that persist even with guidance. HiPO thereby offers a more principled and
 271 efficient path toward mastering complex reasoning.
 272

274 4.2 HOW HiPO CREATES DENSE LEARNING SIGNALS FROM SPARSE REWARDS 275

276 We frame complex reasoning under sparse rewards as a problem of leveraging the structure of suc-
 277 cessful trajectories. However, frequent failures often lead to *signal collapse*, which is a scenario
 278 where zero reward variance within a group nullifies the advantage estimate and halts learning. To
 279 overcome this, HiPO extracts intermediate states from rare successes to serve as “hints” for initiat-
 280 ing new, guided trajectories. This approach transforms the difficult task of end-to-end discovery into
 281 the more manageable one of completing a partially successful reasoning path, generating a dense
 282 learning signal from both unaided and hint-guided rollouts.
 283

284 HiPO’s refines the exploration strategy by modifying the initial state distribution for a subset
 285 of rollouts. We define the set of successful trajectories from the unaided exploration phase as

$$286 \mathcal{T}_{\text{near-miss}}^+ \triangleq \{\tau \in \mathcal{T}_{\text{near-miss}} \mid R(\tau) = 1\}.$$
 287 We define a hint H as an intermediate state s_k within
 288 a successful trajectory, where $s_k \in \tau$ for some $\tau \in \mathcal{T}_{\text{near-miss}}^+$. Trajectories in the Hinted Group, $\mathcal{T}_{\text{hint}}$,
 289 are then generated by sampling from the model π_θ conditioned on the concatenation of an original
 290 prompt P_j and a hint H . This process is formally expressed as $\tau' \sim \pi_\theta(\cdot | P_j \oplus H)$, where H is
 291 a state drawn from a successful trajectory. This acts as a form of value-guided exploration. While
 292 the optimal value function V^* is unknown, states from empirically successful trajectories serve as
 293 effective proxies for high-value states. This method also prevents signal collapse by diversifying re-
 294wards within a batch, which averts the vanishing advantage estimate \hat{A}_τ from identically-rewarded
 295 trajectories. By ensuring signal diversity, HiPO avoids the catastrophic loss of learning signal and
 296 the subsequent stagnation of exploration.
 297

298 To counteract this, HiPO implements a strategic batch replacement. Let $\mathcal{B}_{\text{orig}}$ denote original groups
 299 generated in the unaided exploration. The method sources successful trajectories from $\mathcal{T}_{\text{near-miss}}$
 300 within this batch to generate $\mathcal{T}_{\text{hint}}$. These new groups then strategically replace the $\mathcal{T}_{\text{null-signal}}$ that
 301 offer no learning gradient. This process is formalized as:
 302

$$303 \mathcal{B}_{\text{HiPO}} \triangleq (\mathcal{B}_{\text{orig}} \setminus \mathcal{T}_{\text{null-signal}}) \cup \mathcal{T}_{\text{hint}}. \quad (8)$$

304 The gradient estimator over this optimized batch is:
 305

$$306 \hat{g}_{\text{HiPO}} = \mathbb{E}_{\tau \sim \mathcal{B}_{\text{HiPO}}} \left[\sum_{t=1}^{|\tau|} \nabla_\theta \min \left(r_t^{(\tau)}(\theta) \hat{A}_\tau, \text{clip} \left(r_t^{(\tau)}(\theta), 1 - \epsilon, 1 + \epsilon \right) \hat{A}_\tau \right) \right], \quad (9)$$

307 where \hat{A}_τ is the advantage estimate and $r_t^{(\tau)}$ is the importance sampling ratio. For any trajectory τ
 308 in the augmented batch $\mathcal{B}_{\text{HiPO}}$, its advantage is in its respective group. By replacing, this formula-
 309 tion decomposes the learning objective into a structured set of signals. The gradient is shaped by
 310 four distinct, high-value scenarios. Rare, successful trajectories remaining in $\mathcal{B}_{\text{orig}}$ receive a strong
 311 positive signal, anchoring the policy. In contrast, failed trajectories remaining in $\mathcal{B}_{\text{orig}}$ are penalized,
 312 though their signal may contain “near-miss” paths. Successful trajectories in $\mathcal{T}_{\text{hint}}$ form the core
 313 learning signal by salvaging near-misses from high-value states. Most critically, failed trajectories
 314 in $\mathcal{T}_{\text{hint}}$ provide a clear, high-quality negative signal, precisely penalizing deviations from a known-
 315 good path. By disentangling the learning signal, HiPO effectively transforms the learning problem
 316 from one of sparse rewards and catastrophic signal loss to a structured task of guided completion.
 317

318 5 EXPERIMENTS

319 5.1 EXPERIMENTAL SETTING

320 We train our model on the DAPO dataset (Yu et al., 2025), a challenging collection of 17K mathe-
 321 matical problems with integer answers sourced from the AoPS community. For evaluation, we test
 322 our model across a comprehensive suite of recent mathematics competitions, including the AIME
 323 2024, AIME 2025, BRUMO 2025 (Balunović et al., 2025), HMMT Feb 2025 (Balunović et al.,
 324

2025), CMIMC 2025 (Balunović et al., 2025), and Apex 2025 (Balunović et al., 2025). Performance is measured by the average accuracy across 32 generated samples per problem (avg@32), along with the majority vote accuracy (maj@32) and pass rate (pass@32).

Our approach is based on the Qwen3-8B (Qwen, 2025) model, which we trained our model using the VeRL (Sheng et al., 2024) and using the ReTool framework (Feng et al., 2025; Lin & Xu, 2025). ReTool is a reinforcement learning paradigm that teaches the LLM to utilize a Python code interpreter. It learns from outcome-based feedback over multi-turn interactions, with a maximum of eight turns per math prompt.

Key training hyperparameters include a learning rate of 1e-6, a batch size of 96, a mini-batch size of 12, and a maximum response length of 16K tokens. We adopt the Clip-Higher strategy (Yu et al., 2025), setting ε_{low} to 0.2 and $\varepsilon_{\text{high}}$ to 0.28. At each training step, the policy is updated using rewards calculated from 16 sampled responses per prompt. For evaluation, a maximum response length of 32K tokens is used.

5.2 EMPIRICAL COMPARISON WITH BASELINE

Table 1: Comparison of HiPO, GRPO and DAPO on five benchmarks using avg@32, pass@32, and maj@32. Averages are shown in the last column. Bold indicates the better-performing method for each metric. **For the DAPO, the generation batch size is set to 192, and the maximum number of generation batches is 2.**

Model	AIME 2024			AIME 2025			BRUMO 2025		
	avg@32	pass@32	maj@32	avg@32	pass@32	maj@32	avg@32	pass@32	maj@32
Qwen3-8B	54.7	85.5	60.0	47.6	84.9	63.3	30.3	55.5	56.7
GRPO	72.1	91.7	60.0	63.0	87.1	70.0	41.7	52.1	53.3
DAPO	76.0	89.5	60	63.7	87.9	70	47.8	56.6	63.3
HiPO	76.7	89.8	63.3	66.1	88.3	76.7	46.6	56.6	63.3

Model	HMMT 2025			CMIMC 2025			Average		
	avg@32	pass@32	maj@32	avg@32	pass@32	maj@32	avg@32	pass@32	maj@32
Qwen3-8B	14.0	38.7	40.0	37.0	75.0	60.0	36.7	67.9	56.0
GRPO	28.6	48.2	46.7	43.5	75.0	55.0	49.8	70.8	57.0
DAPO	31.4	48.4	43.3	49.9	80.0	52.5	53.7	72.4	57.8
HiPO	30.8	49.2	40.0	53.8	80.0	65.0	54.8	72.8	61.7

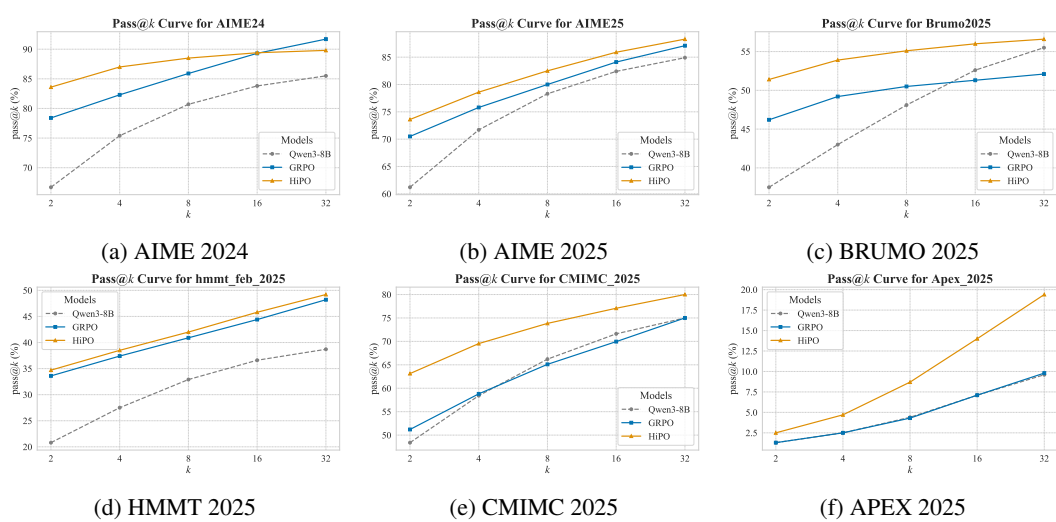


Figure 3: Pass@k curves for different benchmarks.

378 Our experiments demonstrate that HiPO consistently outperforms the GRPO and DAPO (Yu et al.,
 379 2025) baseline on challenging mathematical reasoning benchmarks. As shown in Table 1, HiPO
 380 achieves superior aggregate scores on all primary metrics. Specifically, it obtains an avg@32 of
 381 54.8 compared to GRPO’s 49.8, representing a significant improvement of +5.0 pp. This aggregate
 382 strength is underscored by a notable consistency, as HiPO outperforms GRPO on the avg@32 metric
 383 across all five benchmarks. **Notably, DAPO’s dynamic sampling incurs significant computational**
 384 **overhead, as each training step requires processing a candidate batch of prompts that is a mul-**
 385 **tiple of the size of the batch ultimately used for the gradient update. As shown in Appendix B,**
 386 **DAPO’s dynamic sampling incurs significant computational overhead, consuming approximately**
 387 **4 \times the prompt volume of HiPO to achieve comparable performance.**

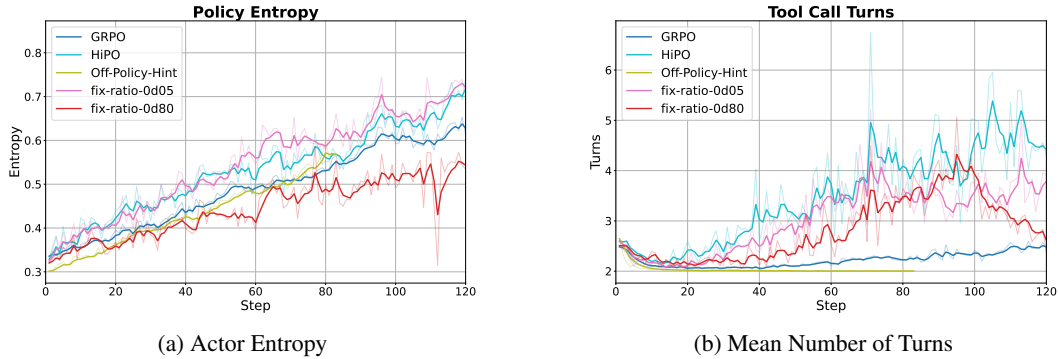
388 The performance disparity is most pronounced on the CMIMC 2025 dataset, where HiPO achieves
 389 a substantial +10.3 pp gain. Further significant improvements are observed on BRUMO 2025
 390 (+4.9 pp) and AIME 2024 (+4.6 pp), underscoring the robustness of HiPO’s advantages. While
 391 GRPO is competitive on certain metrics, HiPO’s consistent and significant lead, particularly on the
 392 most difficult datasets, suggests it learns more robust and generalizable reasoning pathways.

393 These findings are further supported by the pass@k performance (Chen et al., 2021) curves in Fig-
 394 ure 3. The plots generally indicate an advantage for HiPO in sample efficiency, as it often achieves a
 395 higher pass rate at lower values of k . This trend is most pronounced on the exceptionally challeng-
 396 ing Apex 2025 dataset, where the performance gap between HiPO and GRPO widens dramatically
 397 as k increases. On this benchmark, HiPO’s pass@32 score is nearly double that of the baseline,
 398 which suggests that the benefits of its signal reshaping mechanism are particularly salient on prob-
 399 lems where successful trajectories are rare. While the performance of both methods converges at
 400 higher values of k on some benchmarks, such as AIME 2024, HiPO maintains a clear and consistent
 401 performance lead across most other datasets, including Brumo 2025 and AIME 2025, highlighting
 402 the potential robustness of our approach. **Furthermore, we empirically demonstrate HiPO’s robust-**
 403 **ness in ultra-sparse reward regimes by addressing the cold start problem on the hardest subset of the**
 404 **Omni-Math dataset** (Gao et al., 2024) in Appendix C.

405

406 5.3 TRAINING DYNAMICS

407



420 Figure 4: Training dynamics of actor entropy and mean number of turns.
 421

422

423 To understand the mechanisms driving HiPO’s superior performance, we analyze two key metrics
 424 throughout the training process: policy entropy and the average tool-use turns. As plotted in Fig-
 425 ure 4. Figure 4a tracks the policy entropy, a measure of policy stochasticity. The plot shows that
 426 HiPO (cyan) consistently maintains a higher level of entropy than GRPO (blue). This provides
 427 empirical evidence that HiPO successfully mitigates the problem of exploration stagnation (Cui
 428 et al., 2025; Wang et al., 2025). GRPO’s penalization of near-miss trajectories suppresses explo-
 429 ration, causing the policy to converge on suboptimal, low-diversity strategies. In contrast, HiPO’s
 430 on-policy hinting mechanism stabilizes the learning signal, promoting the exploration of diverse
 431 reasoning pathways and preventing premature policy collapse. This sustained diversity is crucial
 432 for discovering more effective problem-solving strategies. The case study in Appendix F provides a
 433 concrete example of this behavioral difference. It shows that the HiPO agent identifies an alterna-

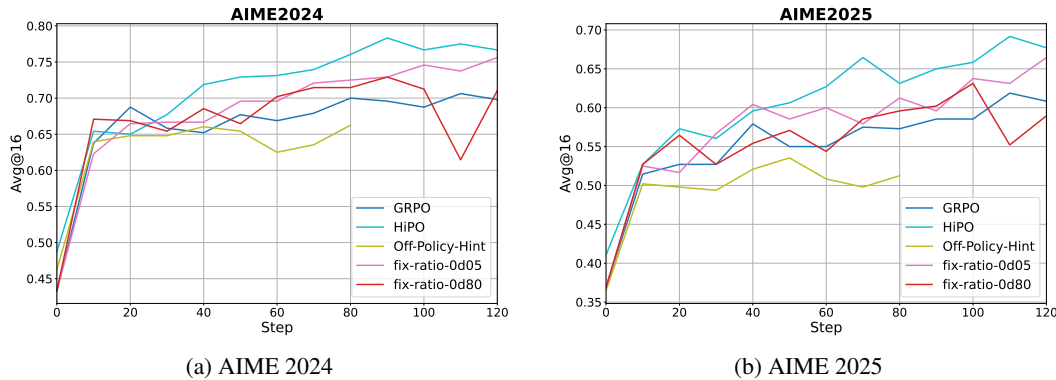


Figure 5: **Ablation on hint ratios.** (a-b) Training curves on AIME 2024 and AIME 2025 benchmarks compared across different hint strategies. (c) The evolution of policy entropy during training. (d) The average number of tool-use turns throughout the training process.

tive algebraic structure to simplify the problem, whereas the GRPO agent follows a more direct but computationally complex path that leads to an incorrect result.

Complementing the entropy analysis, Figure 4b illustrates the model’s capacity for complex, multi-step reasoning by plotting the tool-use turns. A stark divergence emerges: the average number of turns for HiPO trends significantly upwards, indicating that the model learns to engage in longer interactions with the code interpreter. Conversely, the GRPO baseline struggles to increase, showing minimal growth. This suggests that GRPO’s flawed credit assignment makes longer reasoning chains brittle and risky, incentivizing the model to adopt simplistic strategies. HiPO, by providing a scaffold for exploration, enables the model to successfully learn and execute the longer, more complex reasoning chains necessary to solve challenging mathematical problems. Taken together, these dynamics provide compelling evidence that HiPO directly counteracts exploration stagnation. By preserving policy diversity, it enables the model to discover and master the longer, more complex reasoning chains necessary for advanced problem-solving.

5.4 ABLATION STUDY: ANALYSIS OF HINT RATIO

To validate the necessity of our dynamic hint strategy, we evaluate a low-ratio variant with $p = 0.05$ to represent minimal guidance, and a high-ratio variant with $p = 0.80$ to simulate excessive guidance. Figure 5 confirms that HiPO consistently outperforms static hint strategies. The mechanisms driving these results are revealed in the training dynamics. The high-ratio variant ($p = 0.8$) exhibits low entropy and minimal tool-use turns. This indicates that excessive guidance restricts exploration, trapping the model in local sub-optima where it relies on simple completion rather than learning robust reasoning. Conversely, the low-ratio variant ($p = 0.05$) maintains high entropy but fails to increase tool usage. This suggests that while the model is actively exploring, the lack of sufficient scaffolding prevents it from effectively discovering complex, superior trajectories. HiPO achieves the highest tool-use frequency while maintaining healthy entropy, demonstrating that our dynamic strategy successfully strikes a critical balance between exploration and exploitation, guiding the model toward sophisticated solutions without sacrificing diversity.

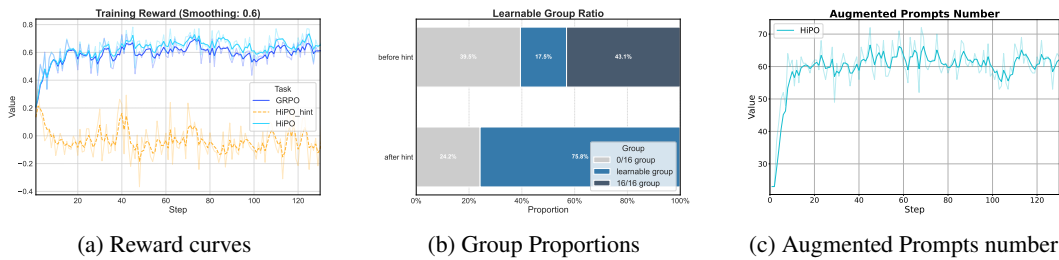
5.5 ABLATION STUDY: ON-POLICY VS. OFF-POLICY HINTS

To determine whether the efficacy of HiPO stems from the content of the hints or the on-policy nature of their generation, we compare HiPO against an “Off-Policy Hint” baseline. We simulate a standard teacher-student distillation by collecting successful trajectories from the base model, extract the first 20% of tokens as static hints.

As shown in Figure 5, the Off-Policy Hint method underperforms both HiPO and the GRPO baseline, a failure explained by the collapse of tool-use turns in Figure 4(b). This collapse occurs

486 because static hints derived from the untrained base model are inherently simplistic. Enforcing these
 487 “weak” priors suppresses exploration, trapping the policy in local optima where it mimics trivial
 488 solutions rather than developing the complex reasoning chains required for harder problems. In
 489 contrast, HiPO establishes a self-reinforcing curriculum where hints evolve dynamically with the
 490 policy. As evidenced by rising tool usage, the “teacher” improves alongside the “student,” enabling
 491 autonomous mastery without reliance on stronger external models.
 492

493 5.6 SAMPLE EFFICIENCY ANALYSIS



504 Figure 6: Visualization of HiPO’s training dynamics. (a) Training reward curves for HiPO and
 505 GRPO. The HiPO_hint curve represents the reward of the new batch after a group substitution occurs.
 506 (b) A bar chart showing the proportion of learnable groups versus ineffective groups within a batch,
 507 before (left) and after (right) applying HiPO. (c) The curve of the number of prompts enhanced by
 508 the HiPO method during training.

509 HiPO is designed to enhance sample efficiency by resolving the “signal collapse” problem endemic
 510 to group-based methods. Our training analysis in Figure 6 empirically confirms this. GRPO wastes
 511 significant computation on “unlearnable groups”, where a staggering 82.5% of all groups (the sum
 512 of 0/16 and 16/16 groups) yield a null gradient. In contrast, HiPO’s hint mechanism transforms these
 513 into valuable learning opportunities. As shown in Figure 6b, HiPO elevates the proportion of learnable
 514 groups to 75.8%. This self-sustaining process remains stable throughout training, evidenced by
 515 a consistently high number of augmented prompts (Figure 6c), which ensures a dense and reliable
 516 learning signal.

517 The impact of this efficiency is evident in the training reward curves shown in Figure 6a. HiPO’s
 518 policy (blue) consistently outperforms the GRPO baseline, demonstrating superior learning. Critically,
 519 this performance gain is achieved on a stable and challenging curriculum. The HiPO hint
 520 curve (orange), which represents the reward of hint-guided rollouts, remains consistently low. This
 521 is a positive signal. It indicates that HiPO continuously forces the model to learn from difficult,
 522 partially-completed trajectories rather than saturating on easy ones. This creates a powerful dynamic
 523 where the model’s overall capability rises (blue curve) while the learning signal remains potent and
 524 challenging (orange curve), ensuring a robust and sustained path to mastery.

526 6 CONCLUSION

528 We addressed the critical challenge of exploration stagnation in RLVR by introducing HiPO, a
 529 framework built on the paradigm of Endogenous Self-Hint. HiPO transforms an agent’s rare,
 530 stochastically-found successes into an on-policy curriculum, converting a sparse reward landscape
 531 into a dense, contrastive learning signal. This self-teaching mechanism not only significantly outper-
 532 formed a strong baseline across challenging reasoning benchmarks but also demonstrably fostered
 533 higher policy entropy and more complex reasoning chains. Our work establishes that a model can
 534 effectively bootstrap its own learning from endogenous successes, reducing the reliance on external
 535 expert data.

536 The principles of HiPO pave the way for a more scalable and autonomous paradigm of skill acquisi-
 537 tion. By demonstrating that models can become active participants in their own education, our work
 538 provides a robust foundation for training self-improving agents capable of mastering intricate tasks
 539 in any domain where success is a rare and hard-won event. This highlights a powerful path toward
 more capable and independent AI.

540 REFERENCES
541

542 Chenxin An, Zhihui Xie, Xiaonan Li, Lei Li, Jun Zhang, Shansan Gong, Ming Zhong, Jingjing
543 Xu, Xipeng Qiu, Mingxuan Wang, and Lingpeng Kong. POLARIS: A post-training recipe for
544 scaling reinforcement learning on advanced reasoning models, 2025. URL <https://hkunlp.github.io/blog/2025/Polaris>.

545

546 Mislav Balunović, Jasper Dekoninck, Ivo Petrov, Nikola Jovanović, and Martin Vechev. MathArena:
547 Evaluating LLMs on uncontaminated math competitions. *arXiv preprint arXiv:2505.23281*, 2025.

548

549 Mark Chen, Jerry Tworek, Heewoo Jun, Qiming Yuan, Henrique Ponde De Oliveira Pinto, Jared
550 Kaplan, Harri Edwards, Yuri Burda, Nicholas Joseph, Greg Brockman, et al. Evaluating large
551 language models trained on code. *arXiv preprint arXiv:2107.03374*, 2021.

552

553 Daixuan Cheng, Shaohan Huang, Xuekai Zhu, Bo Dai, Wayne Xin Zhao, Zhenliang Zhang, and
554 Furu Wei. Reasoning with exploration: An entropy perspective. *arXiv preprint arXiv:2506.14758*,
555 2025.

556

557 Ganqu Cui, Yuchen Zhang, Jiacheng Chen, Lifan Yuan, Zhi Wang, Yuxin Zuo, Haozhan Li, Yuchen
558 Fan, Huayu Chen, Weize Chen, et al. The entropy mechanism of reinforcement learning for
559 reasoning language models. *arXiv preprint arXiv:2505.22617*, 2025.

560

561 Team DeepSeek. DeepSeek-R1 incentivizes reasoning in LLMs through reinforcement learning.
562 *Nature*, 645:633–638, 2025.

563

564 Jiazhan Feng, Shijue Huang, Xingwei Qu, Ge Zhang, Yujia Qin, Baoquan Zhong, Chengquan Jiang,
565 Jinxin Chi, and Wanjun Zhong. ReTool: Reinforcement learning for strategic tool use in LLMs.
566 *arXiv preprint arXiv:2504.11536*, 2025.

567

568 Bofei Gao, Feifan Song, Zhe Yang, Zefan Cai, Yibo Miao, Qingxiu Dong, Lei Li, Chenghao Ma,
569 Liang Chen, Runxin Xu, et al. Omni-math: A universal olympiad level mathematic benchmark
570 for large language models. *arXiv preprint arXiv:2410.07985*, 2024.

571

572 Nathan Lambert, Jacob Morrison, Valentina Pyatkin, Shengyi Huang, Hamish Ivison, Faeze Brah-
573 man, Lester James V Miranda, Alisa Liu, Nouha Dziri, Shane Lyu, et al. Tulu 3: Pushing frontiers
574 in open language model post-training. *arXiv preprint arXiv:2411.15124*, 2024.

575

576 Jiazheng Li, Hong Lu, Kaiyue Wen, Zaiwen Yang, Jiaxuan Gao, Hongzhou Lin, Yi Wu, and
577 Jingzhao Zhang. QuestA: Expanding reasoning capacity in llms via question augmentation. *arXiv
578 preprint arXiv:2507.13266*, 2025a.

579

580 Xuefeng Li, Haoyang Zou, and Pengfei Liu. Torl: Scaling tool-integrated rl. *arXiv preprint
581 arXiv:2503.23383*, 2025b.

582

583 Heng Lin and Zhongwen Xu. Understanding Tool-Integrated Reasoning. *arXiv preprint
584 arXiv:2508.19201*, 2025.

585

586 Team OpenR1. OpenR1-Math-220K: A large-scale dataset for mathematical reasoning., 2025. URL
587 <https://huggingface.co/datasets/open-r1/OpenR1-Math-220k>.

588

589 Martin L Puterman. Markov decision processes. *Handbooks in operations research and management
590 science*, 2:331–434, 1990.

591

592 Team Qwen. Qwen3 technical report. *arXiv preprint arXiv:2505.09388*, 2025.

593

594 Matthew Renze and Erhan Guven. Self-reflection in llm agents: Effects on problem-solving perfor-
595 mance. *arXiv preprint arXiv:2405.06682*, 2024.

596

597 John Schulman, Filip Wolski, Prafulla Dhariwal, Alec Radford, and Oleg Klimov. Proximal policy
598 optimization algorithms. *arXiv preprint arXiv:1707.06347*, 2017.

599

600 Zhihong Shao, Peiyi Wang, Qihao Zhu, Runxin Xu, Junxiao Song, Xiao Bi, Haowei Zhang,
601 Mingchuan Zhang, YK Li, Yang Wu, et al. DeepSeekMath: Pushing the limits of mathemati-
602 cal reasoning in open language models. *arXiv preprint arXiv:2402.03300*, 2024.

594 Guangming Sheng, Chi Zhang, Zilingfeng Ye, Xibin Wu, Wang Zhang, Ru Zhang, Yanghua Peng,
595 Haibin Lin, and Chuan Wu. HybridFlow: A flexible and efficient RLHF framework. *arXiv*
596 *preprint arXiv: 2409.19256*, 2024.

597 Richard S Sutton and Andrew G Barto. *Reinforcement learning: An introduction*. MIT press, 2018.

598 Shenzhi Wang, Le Yu, Chang Gao, Chujie Zheng, Shixuan Liu, Rui Lu, Kai Dang, Xionghui Chen,
599 Jianxin Yang, Zhenru Zhang, et al. Beyond the 80/20 rule: High-entropy minority tokens drive
600 effective reinforcement learning for LLM reasoning. *arXiv preprint arXiv:2506.01939*, 2025.

601 Zhongwen Xu and Zihan Ding. Single-stream policy optimization. *arXiv preprint*
602 *arXiv:2509.13232*, 2025.

603 Qiying Yu, Zheng Zhang, Ruofei Zhu, Yufeng Yuan, Xiaochen Zuo, Yu Yue, Weinan Dai, Tiantian
604 Fan, Gaohong Liu, Lingjun Liu, et al. DAPO: An open-source LLM reinforcement learning
605 system at scale. *arXiv preprint arXiv:2503.14476*, 2025.

606 Kaiyi Zhang, Ang Lv, Jinpeng Li, Yongbo Wang, Feng Wang, Haoyuan Hu, and Rui Yan.
607 StepHint: Multi-level stepwise hints enhance reinforcement learning to reason. *arXiv preprint*
608 *arXiv:2507.02841*, 2025.

609
610
611
612
613
614
615
616
617
618
619
620
621
622
623
624
625
626
627
628
629
630
631
632
633
634
635
636
637
638
639
640
641
642
643
644
645
646
647

A LLM USAGE

We used large language models (LLMs) only to polish grammar and improve the clarity of the manuscript. All research ideas, experiments, and analyses were conducted by the authors.

B COMPARISON WITH DAPO

We compare HiPO against DAPO (Yu et al., 2025), a strong baseline employing dynamic sampling to tackle sparse rewards. To accurately reflect computational cost, Figure 7 evaluates performance against prompt volume.

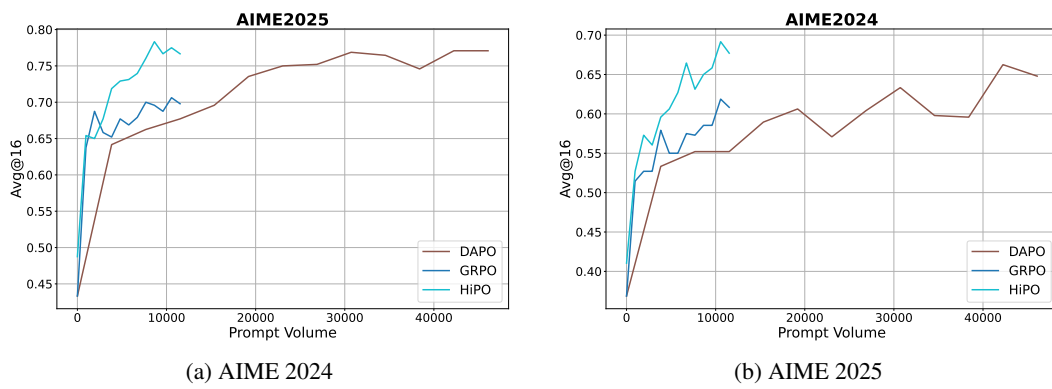


Figure 7: Performance curves (Avg@16) on AIME 2024 (a) and AIME 2025 (b) plotted against the total Prompt Volume. The trajectories correspond to GRPO (blue), HiPO (cyan), and DAPO (brown).

As shown in Figure 7, HiPO achieves superior convergence with a fraction of the data consumption. The extended tail of DAPO reveals the high cost of its dynamic sampling mechanism: to secure positive rewards, it must perform extensive rejection sampling, consuming approximately $4\times$ the trajectory budget per update step. While DAPO relies on brute-force enumeration to locate sparse successes, HiPO employs signal amplification. By repurposing a single stochastic success into a group-wide hint, HiPO extracts dense gradients from standard batches, eliminating the need for wasteful resampling and establishing a significantly more efficient learning paradigm.

C ROBUSTNESS TO ULTRA-SPARSE REWARDS

A primary concern regarding RLVR in complex domains is the “cold start” problem, where ultra-sparse rewards might starve the model of learning signals. To empirically evaluate HiPO’s robustness in such regimes, we conducted a stress test using the top 10% most difficult problems from the Omni-Math dataset (Gao et al., 2024) to train a Qwen3-8B base model. This setup simulates a near-zero success rate environment where standard exploration often stagnates.

The results in Figure 8 demonstrate that HiPO effectively mitigates signal scarcity through batch-level signal broadcasting. As illustrated in Figure 8(a), the initial generation phase (blue bars) is dominated by groups with zero successes, which would typically yield a null gradient. However, HiPO identifies rare stochastic successes present within the global batch and repurposes them to generate hinted groups. The cyan bars show a drastic reduction in these unlearnable groups after intervention, indicating that the method effectively amplifies sparse signals by substituting failed trajectories with actionable, hint-guided ones. This mechanism ensures that even when success is statistically rare, the optimization process remains supplied with valid gradients. Figures 8(b) and (c) confirm that this signal rectification translates into tangible learning progress, with the model

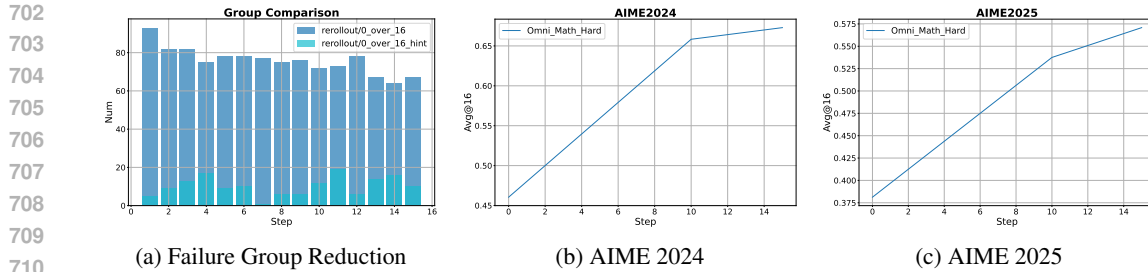


Figure 8: HiPO in Ultra-Sparse Regimes (Omni-Math-Hard). (a) The number of “Total Failure” groups (0/16 success) in a batch before (Blue) and after (Cyan) HiPO intervention. HiPO drastically reduces the proportion of null-signal groups. (b-c) Despite the extreme difficulty, the model maintains a steady upward learning trend on AIME benchmarks, confirming that the feedback loop remains unbroken.

maintaining a steady upward trend on both AIME 2024 and AIME 2025 benchmarks despite the extreme difficulty of the training distribution.

D RANDOM HINT SETTING

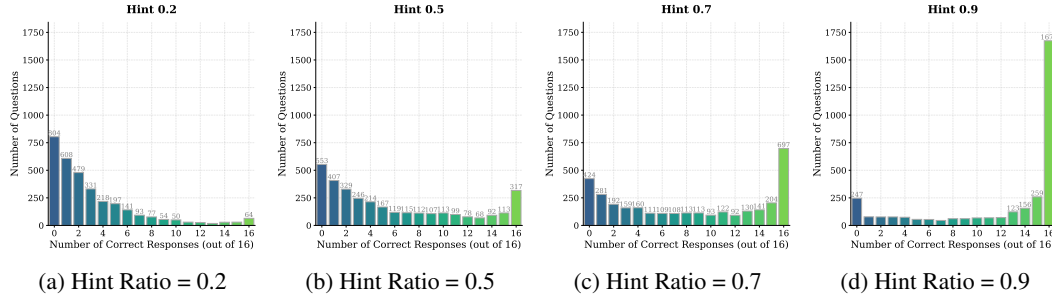


Figure 9: Distribution of the number of correct responses over 16 attempts ($n/16$) for different fixed hint ratios. These plots illustrate how increasing the hint ratio shifts the distribution towards perfect scores, inadvertently creating less effective learning signals.

As empirically demonstrated in Figure 9, hint ratios exceeding 0.5 cause a sharp increase in the frequency of perfect-score (16/16) groups. This outcome is detrimental because it induces “signal collapse.” In a group where all trajectories succeed, the reward variance is zero, which nullifies the advantage estimate ($\hat{A}_{j,i} = 0$) for all samples and causes the policy gradient to vanish. Furthermore, excessively long hints reduce the problem to a trivial completion task, preventing the model from learning the complex intermediate reasoning steps and suppressing meaningful exploration of the solution space.

Using a single, fixed hint ratio creates a critical credit assignment pathology, which can be shown formally. Consider a hinted group $T_j = \{\tau_{j,1}, \dots, \tau_{j,n}\}$ where all trajectories share an identical prefix $H = (o_0, \dots, o_{k-1})$ because they are derived from a single source trajectory with a fixed ratio. In GRPO, the total policy gradient for any token o_t within this shared prefix ($t < k$) is the sum of its gradients from each trajectory in the group. Since the advantage $\hat{A}_{j,i}$ is constant for all tokens within a trajectory $\tau_{j,i}$, and the conditional probability $\pi_\theta(o_t|s_t)$ is identical for all trajectories at this step, the total gradient for token o_t is:

$$\nabla_\theta J(o_t) = \sum_{i=1}^n \hat{A}_{j,i} \nabla_\theta \log \pi_\theta(o_t|s_t) = \left(\sum_{i=1}^n \hat{A}_{j,i} \right) \nabla_\theta \log \pi_\theta(o_t|s_t). \quad (10)$$

The core issue lies in the summed advantage term. By definition, the advantage $\hat{A}_{j,i} = (R(\tau_{j,i}) - \mu_{\tau_j})/(\sigma_{\tau_j} + \epsilon)$, where μ_{τ_j} is the mean reward of the group. The sum of all advantages within the

group is therefore:

$$\sum_{i=1}^n \hat{A}_{j,i} = \frac{1}{\sigma_{\tau_j} + \epsilon} \sum_{i=1}^n (R(\tau_{j,i}) - \mu_{\tau_j}) = \frac{1}{\sigma_{\tau_j} + \epsilon} \left(\left(\sum_{i=1}^n R(\tau_{j,i}) \right) - n \cdot \mu_{\tau_j} \right) = 0. \quad (11)$$

This demonstrates that the aggregate advantage signal for any token in the shared prefix is precisely zero, resulting in a null gradient. The model is thus unable to learn that the shared prefix is a valuable reasoning path. Randomly sampling the hint ratio breaks this pathological symmetry by ensuring the prefixes are not identical, which allows for a meaningful, non-zero gradient to be assigned.

E GENERALIZATION TO OUT-OF-DISTRIBUTION TASKS

We evaluated HiPO on HumanEval to assess its generalization capabilities beyond the mathematical domain. Despite the training data consisting exclusively of mathematical problems—making code generation a fully out-of-distribution (OOD) task, HiPO achieves a Pass@1 score of 71.3%, outperforming the Qwen3-8B base model (70.7%). This demonstrates that the enhanced reasoning patterns fostered by HiPO are robust and transferable, yielding performance improvements even on tasks unseen during training.

Table 2: Pass@1 (%) on the HumanEval benchmark. HiPO demonstrates positive generalization on this OOD coding task, outperforming the base model.

Model	Pass@1
Qwen3-8B (Base)	70.7
GRPO	71.3
HiPO (Ours)	71.3

F CASE STUDY

To provide a concrete illustration of the behavioral differences between HiPO and the GRPO baseline, we present a qualitative case study. The following Table 3, Table 4 and Table 5 contrasts the reasoning trajectories of both models on a challenging mathematical problem that requires both insight and precise execution. This side-by-side comparison highlights HiPO’s ability to perform strategic exploration to simplify the problem’s core, versus GRPO’s tendency to get locked into a linear, computationally intensive, and ultimately fragile reasoning path.

As the comparison demonstrates, HiPO's ability to perform strategic exploration leads to a more robust and efficient solution path. In contrast, the baseline model's linear, brute-force approach results in a fragile reasoning chain that ultimately collapses due to its own complexity, perfectly illustrating the "exploration stagnation" that our method is designed to overcome.

810
811
812
813
814
815
816
817
818
819
820
821

822 Table 3: A second comparative case study. This table illustrates HiPO’s strategy of leveraging
823 external tools (a code interpreter) to definitively verify its algebraic insight. In contrast, the GRPO
824 baseline performs a robust but purely algebraic verification, re-solving the problem with a different,
825 more complex method to ensure correctness.

[Question]	
HiPO Trajectory (Our Method)	GRPO Trajectory (Baseline)
<p>826 827 828 829 830 831 832 833 834 835 836 837 838 839 840 841 842 843 844 845 846 847 848 849 850 851 852 853 854 855 856 857 858 859 860 861 862 863</p> <p>Positive real numbers x and y satisfy $y^3 = x^2$ and $(y - x)^2 = 4y^2$. What is $x + y$?</p> <p>Response: ...Wait, $(y - x)^2 = 4y^2 \rightarrow$ taking square roots gives $y - x = 2y$. ...Case 1: $y - x = 2y \rightarrow x = -y$. But x and y are positive, so this can’t be possible... Case 2: $y - x = -2y \rightarrow x = 3y$. So from this, x equals $3y$. Now, substitute this into equation 1. $y^3 = (3y)^2 \rightarrow y^3 = 9y^2 \rightarrow y = 9$. So $y=9$. Then $x=3y=27$. Therefore, $x + y = 27 + 9 = 36$.</p> <p>But perhaps the code can solve this system of equations.</p> <pre>import sympy as sp x, y = sp.symbols('x y', positive=True) eq1 = sp.Eq(y**3, x**2) eq2 = sp.Eq((y - x)**2, 4*y**2) solution = sp.solve((eq1, eq2), (x, y)) result = solution[0][0] + solution[0][1] # result is 36</pre> <p>Yes, the code gives 36. So that confirms the answer. The final answer is 36.</p>	<p>826 827 828 829 830 831 832 833 834 835 836 837 838 839 840 841 842 843 844 845 846 847 848 849 850 851 852 853 854 855 856 857 858 859 860 861 862 863</p> <p>Response: ...Let’s take the square root of both sides... we get $y - x = 2y$. ...Case 1: $y - x = 2y \rightarrow x = -y$. But x and y are positive, so this is impossible. Case 2: $y - x = -2y \rightarrow x = 3y$. So this is the valid case. Substitute $x = 3y$ into... $y^3 = (3y)^2 \rightarrow y^3 = 9y^2$. ...so $y = 9$. Then $x = 3y = 3 \times 9 = 27$. Therefore, $x + y = 27 + 9 = 36$.</p> <p>Wait, but let me check again if there’s another way to approach this... Alternatively, maybe expanding equation 2. $(y - x)^2 = y^2 - 2xy + x^2 = 4y^2$. ...$x^2 - 2xy - 3y^2 = 0$. Let me treat this as a quadratic equation in x... Using quadratic formula: $x = [2y \pm \sqrt{(2y)^2 - 4(1)(-3y^2)}]/2$ $x = [2y \pm \sqrt{16y^2}]/2 = [2y \pm 4y]/2$. ...only $x = 3y$ is valid. So same result as before. So that’s correct. All approaches lead to $x=27$, $y=9$, sum 36. The final answer is 36.</p>

864
865
866
867
868
869
870
871
872
873
874
875

Table 4: A case study in problem restructuring. The HiPO trajectory shows the use of a key algebraic insight to simplify the problem’s structure, leading to a straightforward solution. In contrast, the baseline’s linear approach gets entangled in more complex and error-prone calculations.

[Question]	
HiPO Trajectory (Our Method)	GRPO Trajectory (Baseline)
<p>876 877 878 879 880 881 882 883 884 885 886 887 888 889 890 891 892 893 894 895 896 897 898 899 900 901 902 903 904 905 906 907 908 909 910 911 912 913 914 915 916 917</p> <p>Find the number of triples of nonnegative integers (a, b, c) satisfying $a + b + c = 300$ and</p> $a^2b + a^2c + b^2a + b^2c + c^2a + c^2b = 6,000,000.$ <p>Response: ...This leads to the relation ‘$abc - 100(ab + bc + ca) = -2,000,000$’.</p> <p>This seems a bit abstract. How can I proceed from here?</p> <p><i>Alternatively, maybe think of the left-hand side as $(a-100)(b-100)(c-100)$?</i> ...</p> $(a - 100)(b - 100)(c - 100) = 0.$ <p>Oh! That’s a big simplification! ...This is a counting problem I can solve with inclusion-exclusion.</p> <p>Number of solutions is: $3 \times 201 - 3 \times 1 + 1 = 601$.</p> <p>But to make sure, perhaps code it.</p> <pre> def count_solutions(): # Solutions where a=100: b+c =200 -> 201 count = 3 * 201 # Subtract overlaps where a=b =100 count -= 3 # Add back the case where a=b=c =100 count += 1 return count print(count_solutions()) </pre> <p>Interpreter Output: 601</p> <p>The code confirms my reasoning. The final answer is 601.</p>	<p>Find the number of triples of nonnegative integers (a, b, c) satisfying $a + b + c = 300$ and</p> $a^2b + a^2c + b^2a + b^2c + c^2a + c^2b = 6,000,000.$ <p>Response: ...This leads to the relation ‘$abc - 100(ab + bc + ca) = -2,000,000$’.</p> <p>But how can I proceed from here? Let me think.</p> <p>Let me check the case where one variable is zero first... This gives 6 solutions.</p> <p>Now, let me think about other cases...</p> $P'(c - 100) = -100(c^2 - 300c + 20000).$ <p>Let me factor the right-hand side...</p> $P'(c - 100) = -100(c - 200)(c - 100).$ <p>...The discriminant is $D = (S' - 200)^2$, which is a perfect square. Exactly!</p> <p>...So for each c from 1 to 199, there are two ordered triples... except $c = 100$. So total solutions is $1 + 198 \times 2 = 397$.</p> <p>Wait, this is a critical point... This is a big mistake in the earlier reasoning...</p> <p>The total number of solutions is $6 + 397 = 403$. The final answer is 403.</p>

918
919
920
921
922
923
924
925
926
927
928
929

Table 5: A case study on strategy selection. HiPO correctly identifies the problem as best suited for a computational brute-force search, leading to the correct answer. The baseline attempts a more complex analytical shortcut, but a subtle reasoning error leads to an incorrect result, highlighting the robustness of HiPO’s strategy.

930
931
932
933
934
935
936
937
938
939
940
941
942
943
944
945
946
947
948
949
950
951
952
953
954
955
956
957
958
959
960
961
962
963
964
965
966
967
968
969
970
971

[Question]	
HiPO Trajectory (Our Method)	GRPO Trajectory (Baseline)
<p><i>Response:</i></p> <p>Okay, I need to solve this problem... For a number to have exactly two digits in base b, it must satisfy $b \leq n < b^2$. Let the digits be d_1 and d_2. Then $n = d_1 \cdot b + d_2$ and $d_1 + d_2 = \sqrt{n}$.</p> <p>So the plan is: For each base b starting from 2 upwards... iterate over all possible d_1 and d_2... check if $(d_1+d_2)^2 == n$... and count them. This seems suitable for code.</p> <pre> def find_min_base(): b = 2 while True: count = 0 for d1 in range(1, b): for d2 in range(0, b): n = d1 * b + d2 sum_d = d1 + d2 if sum_d * sum_d == n: count += 1 if count > 10: return b b += 1 result = find_min_base() print(result) </pre> <p>Interpreter Output: 211</p> <p>Wait, the code returns 211? That seems high.</p> <p>Let me check for $b=3$. $d_1=1, d_2=1$: $n=4$, $\text{sum}=2$. $2^2=4$. Yes. ...other pairs fail. So for $b=3$, count is 1. The code logic seems to be working. So the answer is 211.</p>	<p><i>Response:</i></p> <p>Okay, let’s tackle this problem... Let $n = a \cdot b + c$. The condition is $\sqrt{ab + c} = a + c$. Let $s = a + c$. Then $s^2 = ab + (s - a)$, which gives $a = \frac{s(s-1)}{b-1}$.</p> <p>For a to be an integer, $b-1$ must divide $s(s-1)$. Since s and $s-1$ are coprime, $b-1$ must divide s or $s-1$.</p> <p>...This seems to imply there are very few solutions for any b.</p> <p>Wait, let me check the example. $b=13, n=81$. Digits are 6, 3. $s=9$. $b-1=12$. Here, $s(s-1) = 9 \times 8 = 72$. 12 divides 72, but 12 does not divide 9 or 8. Ah! My reasoning was incorrect. So I need to check for each s if $b-1$ divides $s(s-1)$. Let me try to code this.</p> <pre> # Tries to write code # ... but it has syntax errors def count_beautiful(b): #... # ... code fails to run </pre> <p>At this point, it’s clear that without writing the code, it’s hard to proceed. Let me try to estimate for $b=61$... This is getting too complex. The answer is 121.</p>